Neural Processing Letters (2023) 55:229–245
https://doi.org/10.1007/s11063-021-10571-1

AI-Based Self-Learning System in Distributed Structural Health Monitoring and Control

Kai Yan[1] · Xin Lin[1] · Wenfeng Ma[1] · Yuxiao Zhang[1]

Accepted: 24 June 2021 / Published online: 25 August 2021

Abstract
Artificial intelligence is predicted to play a big part in self-learning, industrial automation that will negotiate the bandwidth of structural health and control systems. The industrial structural health and control system based on discrete sensors possesses insufficient spatial coverage of sensing information, while the distributed condition monitoring has been mainly studied at the sensor level, relatively few studies have been conducted at the artificial intelligence level. This paper presents an innovative method for distributed structural health and control systems based on artificial intelligence. The structural condition was divided into regional and local features, the feature extraction and characterization are performed separately. Structural abnormality recognition and risk factor calculation method were proposed by considering the response values and the distribution patterns of both the regional and the local structural behaviours. The test results show that the method can effectively identify the full-scale and local damage of the structure, respectively. Subsequently, structural safety assessment method for long-span structures at kilometres level in view of fully length strain distributions measured by distributed fiber optic sensors were developed. A series of load tests on the long-span structure were carried out. Finite element (FE) model was developed using finite element code, ABAQUS, and an extensive parametric study was conduct to explore the effect of load cases on the structural responses. The differences in the structural response results among load test, structural safety assessment and FE simulation were investigated. It is shown that AI-based self-learning system could offer suitable speed in deployment, reliability in solution and flexibility to adjust in distributed structural health monitoring and control.

Keywords Artificial intelligence · Structural control system · Distributed fiber optic · Abnormality recognition · Pattern matching method

✉ Kai Yan
yankai@sdjzu.edu.cn

[1] Key Lab of Building Structural Retrofitting and Underground Space Engineering of the Ministry of Education, Shandong Jianzhu University, Jinan, China

1 Introduction

The portable wireless technologies offer an attractive opportunity for distributed control systems, especially for AI-based self-learning in mass information processing of structural health monitoring and control. Civil infrastructures are costly and carry major tasks of people's life, social development, and economic construction. The service life of the infrastructures spans decades and even hundreds of years. During the service period, due to the coupling effect of catastrophic factors such as environment and load, fatigue effects, corrosion effects, and aging of materials, the structure inevitably generates damage accumulation and resistance attenuation, thereby the ability to resist natural disasters reduces. Once it fails, it is economic The loss and social impact are extremely severe [1]. In severe cases, civil infrastructures might be notable damaged or even collapse, causing a lot of casualties and properties loss. With the characteristics of long service life, harsh service environment, complex failure laws and serious damage consequences, safe service and maintenance for civil infrastructures should be ensured in full life cycle [2, 3]. Structural safety monitoring and decision methods, containing monitoring the real response, damage and performance degradation of structural services, and assessing the structural safety status, have been proposed and studied in the past 30 years [4–8]. The traditional structural safety monitoring method has the problem of insufficient spatial coverage of sensory information [9]. Moreover, new structural safety monitoring methods based on large-scale spatial coverage and dense sensory information has been mainly studied at the sensing technology level, and relatively few studies have been conducted at the system level [10–12]. Recently, high-performance distributed optical fiber sensing technology on artificial intelligent brillouin time domain analysis (BOTDA) system is developing rapidly. The artificial intelligent BOTDA system can endue civil infrastructures a full-scale perception and gather the true strain response distribution of the whole structure. Due to ultra-long sensing distance, distributed, high-density measurement, outstanding durability, the development and applications of BOTDA system has been widely spread in bridges, long span structures, civil buildings, coastal structures and defense engineering [13–17]. From the perspective of the overall structural safety monitoring system, global strain information is essential foundation for revealing the structural behavior, while, structural damage identification, safety status assessment and smart safety decision system based on distributed structural behaviors need to be further improved for civil infrastructures.

Distributed sensing technologies for the safety of civil infrastructures are divided into two categories, one is quasi-distributed sensing technology, such as fiber grating multiplexing technology. Multiple gratings are engraved on one sensing fiber, and the sensing information of all the gratings can be demodulated at the same time by wavelength division multiplexing or time division multiplexing [18]. One signal transmission line is needed, which only takes up one sensing channel and one optical fiber. The number of gratings connected in series can reach dozens. Due to the low signal transmission loss of the optical fiber, the sensing length can reach tens of kilometers [19–22]. Quasi-distributed sensing technology possesses the advantages of simple structure, good durability, accurate testing, strong dynamic testing ability, and mature technology. While the limited space coverage, low dense sensing points, and high cost of large-scale reuse are also obvious on the sensing technology. The other is fully distributed sensing technology, such as distributed fiber sensing technology based on stimulated Brillouin scattering. It employs ordinary single-mode fiber as a sensor, demodulates the distributed strain and temperature from the Brillouin scattered light in the fiber. The fiber is both a sensor and a signal transmission line. The use

of BODTA system in civil infrastructures can realize the full-scale coverage monitoring, with a sensing distance exceeding 150 km [23, 24]. This smart system has high-density distributed sensing on strain and temperature, with the number of sensing points upper hundreds of thousands and the distance between adjacent sensing points under 1 cm. The volume of the optical fiber is slim and flexible to install. The diameter of the bare fiber is 12.5 μm, and the packaged optical cable is mostly less than 5 mm [17]. On the structure geometry, comprehensive sensing information of the tested structure can be obtained by the high flexibility sensor.

The safety monitoring and evaluation of civil infrastructures increasingly become an effective method for research on damage evolution behaviour and an important operational safety guarantee technology. However, although structural safety monitoring has been applied in some practical projects, the theoretical research and application of structural safety monitoring is still in its infancy [25]. Most of the monitoring systems installed in practical projects use traditional sensors. It is worth noting that the structural damage identification is also mainly based on the identification of structural dynamic characteristics. As the core content of safety monitoring, damage identification and localization are urgently needs to be resolved [26]. BOTDA technology can solve the problem of structural damage identification and localization in the sensor hardware level by global distributed strain measurement.

At present, BOTDA technology has not been widely used in safety of monitoring civil infrastructures, with the main reason that the combination of this technology and civil infrastructural monitoring still has some technical bottlenecks to be broken. As a sensor for long distance measurement, the measurement accuracy of is BOTDA relatively low [27]. The nominal strain test accuracy of the system is usually 20με, and due to the test features of spatial resolution, the test results are affected by the measured strain field inhomogeneity, which will introduce additional errors [28]. The negative effects of low measurement accuracy and the additional errors might lead to the distorted result [29]. Compared with the point precision strain sensor, there is still a large gap in test accuracy and spatial resolution. The measurement of BOTDA is quasi-real-time monitoring. It usually takes tens of seconds to several minutes to complete a measurement, so only static measurement can be performed, and the dynamic response of the measured structure cannot be accurately obtained [30]. The main technical advantage of BOTDA is long-distance and dense distributed measurement. While, most of the current international studies focus on small structures and structural members, and the performance of BODTA in the safety monitoring of large structures need further engineering practice verification. More importantly, according to author's knowledge, the new structural health monitoring methods based on large-scale spatial coverage and dense sensing information has been rarely studied. In the actual monitoring of large structures, due to the complex factors of actual structures, the interpretation of data from BOTDA is obviously more difficulty than that of small structures and laboratory tests. Therefore, it is necessary to develop a safety decision system of in-depth data interpretation to dig out valuable structural status information and corresponding safety evaluation.

This paper presents an innovative method for distributed structural health and control systems based on artificial intelligence. AI-based self-learning method was employed to improve the mass information process. The structural condition was divided into regional and local features, the feature extraction and characterization are performed separately. Structural abnormality recognition and risk factor calculation method were proposed by considering the response values and the distribution patterns of both the regional and the local structural behaviours. It is shown that the structural safety assessment method is

scientific and reliable for structural health monitoring using distributed sensors. The results shows that AI-based self-learning system could offer suitable speed in deployment, reliability in solution and flexibility to adjust in distributed structural health monitoring and control.

2 AI-Based Self-Learning System in Distributed Structural Health Monitoring

The distributed optical fiber measurement results represent the state parameter values of various locations of the structure under test, such as temperature values or strain values. On the other hand, due to long-distance, distributed, and highly dense measurement points, its measurement results also include information on the distribution pattern of the structural state parameters. Therefore, compared to point measurement methods, distributed optical fiber can obtain more locations and more structural status information of civil infrastructures. The classification and extraction of structural state characteristic information contained in distributed optical fiber monitoring data is an important basis for structural state assessment.

2.1 Measurement Characteristics of AI-Based Self-Learning System

There are three types of scattering effects that occur when light travels through an optical fiber. As shown in Fig. 1, they are Rayleigh scattering caused by changes in the refractive index of the fiber, Raman scattering caused by optical phonons, and Abyssal scattering. Brillouin scattering is a non-linear scattering effect, that is, the Brillouin scattered light has a certain offset from the frequency of the incident light. This frequency offset is called the Brillouin frequency shift v_a of the fiber. According to different excitation states, Brillouin scattering in optical fiber is divided into two types: self-published Brillouin scattering and stimulated Brillouin scattering. Stimulated Brillouin scattering is the measurement basis of BOTDA system.

The mechanism of stimulated Brillouin scattering in an optical fiber is shown in Fig. 2. The two laser beams transmitted in the opposite direction are the high-frequency pump

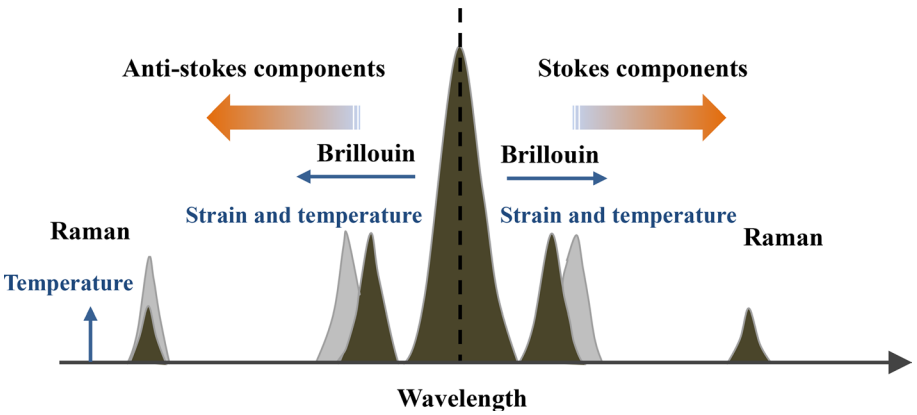

Fig. 1 The backscattered components of light in an optical fiber

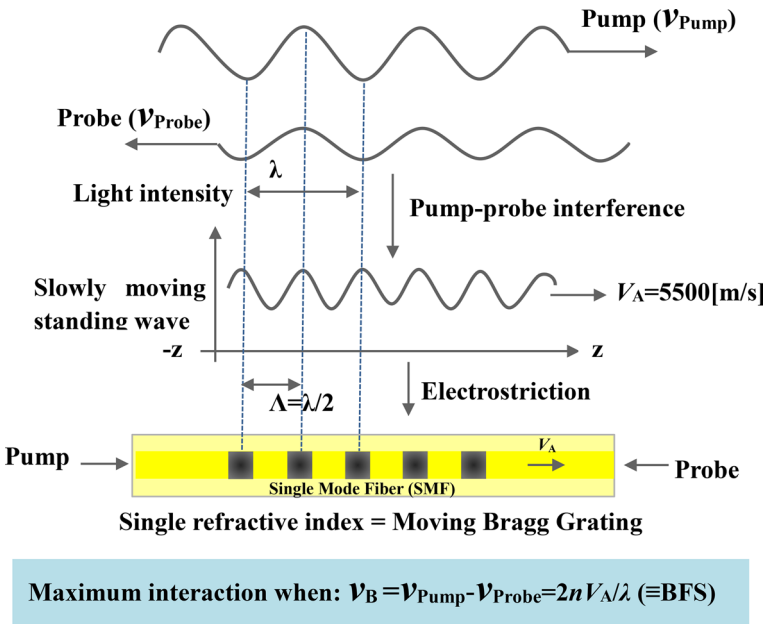

Fig. 2 Principles of stimulated Brillouin scattering

light (v_{pump}) and the low-frequency probe light (v_{probe}), which meet in the optical fiber and cause interference effects, and generate a periodic wave of light intensity with a frequency of pump. The difference between the frequency of pump light and probe light, that is, $V_A = v_{pump} - v_{probe}$. The inherent properties of the fiber material cause a certain form of vibration at the micro level, causing the density of the fiber to fluctuate periodically with time and space, resulting in the fiber spontaneous acoustic wave field with a moving speed of V_A and a frequency of V_B. The relationship between the fiber Brillouin frequency shift V_B and the spontaneous acoustic wave field velocity V_A is $V_B = 2n\ V_A/\lambda$. where n is the wavelength of the pump light. When the frequency difference between the pump light and the probe light is equal to the Brillouin frequency shift of the optical fiber, the acoustic wave field generated by the interaction between the two will completely match the spontaneous acoustic wave field of the optical fiber, causing resonance effects, resulting in the intensity of the optical sound field significantly enhanced, the efficiency of the pump light to the detection light energy sensing is greatly improved, and the detection light will show a significant intensity gain signal.

BOTDA distributed fiber sensing technology utilizes stimulated Brillouin scattering effect to realize distributed measurement of strain and temperature. The sensing principle is shown in Fig. 3. Two oppositely transmitted laser beams are simultaneously injected at both ends of the sensing fiber. The two laser beams meet in the optical fiber and a stimulated Brillouin scattering effect occurs. The Brillouin gain signal is obtained by continuously detecting the light. The peak of the Brillouin gain spectrum represents the maximum intensity gain generated by pumped and probed light with stimulated Brillouin scattering. The frequency difference between the two corresponding to the peak position is the Brillouin frequency shift of the sensing fiber. Through this method, a Brillouin frequency shift distribution at each position of the entire length of the sensing fiber can be obtained.

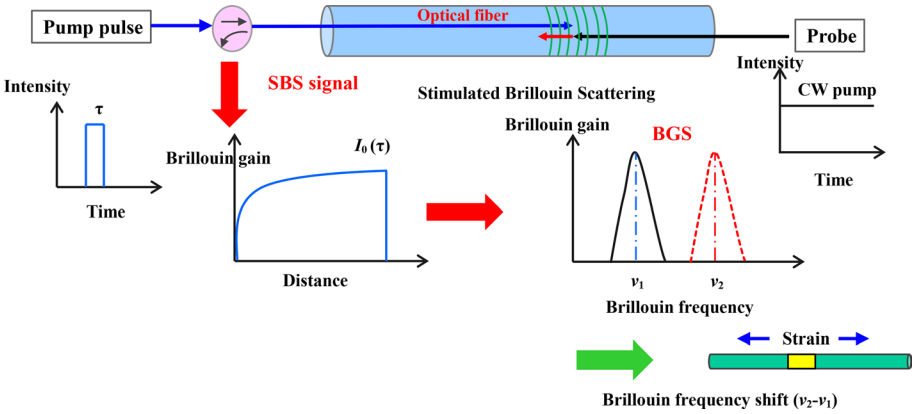

Fig. 3 Principles of an AI-based self-learning system

The Brillouin frequency shift of an optical fiber is sensitive to the changes in temperature and strain of the optical fiber, and the relationship is:

$$V_B = V_{B0} + C_s(\varepsilon - \varepsilon_0) + (t - t_0) \tag{1}$$

where ε_0, t_0 and V_{B0} are the strain, temperature, and Brillouin frequency shift of the sensing fiber in the initial state; ε, t and V_B are the strain, temperature, and Brillouin frequency shift of the sensor fiber in the measurement state. C_s and C_t are scale factor. The temperature and strain distribution of the sensing fiber can be obtained by Formula 1.

2.2 Extraction and Characterization of the Regional/Local Structural Behaviour

The structural state distribution data measured by distributed optical fibers includes two types of distribution features, regional distribution features and local distribution features, which need to be extracted and characterized separately. Let the measurement point position vector of the distributed optical fiber monitoring result be $\mathbf{X}$ and the structural state vector be $\mathbf{S}$. The expressions of the two vectors are $\mathbf{X}=(x_1, x_2, \ldots, x_N)$, $\mathbf{S}=(s_1, s_2, \ldots, s_N)$. x_i represents the structural position corresponding to the i-th measuring point ($i=1, 2, \ldots, N$). s_i represents the measurement value of the structural state parameter at the position x_i, and the total number of measurement points of the distributed optical fiber system is N.

Let the length of the distribution feature extraction window be w_a. w_a is a positive integer and satisfies the condition, $w_a \geq w/\Delta x$. w is the spatial resolution length of the distributed optical fiber measurement system, and $\Delta x = x_i - x_{i-1}$ is the measurement point interval. Taking w_a as the window length and Δx as the moving step size, moving average of the structural state vector $\mathbf{S}$ is separated into a regional state distribution vector $\mathbf{r}$ and a local state distribution vector $\mathbf{L}$:

$$\mathbf{r} = (r_1, r_2, \ldots, r_N) \tag{2}$$

$$\mathbf{L} = (l_1, l_2, \ldots, l_N) \tag{3}$$

$$l_i = s_i - r_i, \quad i = 1, 2, \ldots, N \tag{4}$$

$$r_i = \frac{1}{w_a} \sum_{t=i-\Delta w_a}^{i-\Delta w_a+w_a-1} s_t, \quad i = 1, 2, \ldots, N \tag{5}$$

r_i represents the average value of the structural state of the sensing fiber in the region $x_{i\text{-}\Delta wa}$ to $x_{i\text{-}\Delta wa+wa-1}$, and $\mathbf{r}$ reflects the overall state distribution characteristics of the structure. l_i represents the difference between the structural state of the sensing fiber at the position x_i and the average of the structural state in the region. $\mathbf{L}$ reflects the local state distribution characteristics of the structure.

2.3 Pattern Matching Method for Evaluating Structural Response Distributions

A single structural state distribution pattern cannot reflect the change of structural state. At least two structural state distribution patterns must be compared to find out the abnormal position of the distribution pattern and evaluate the degree of abnormality in order to perform an effective structural state assessment. Let the reference state distribution vector be $\mathbf{S_{ref}}$ and the evaluation state distribution vector be $\mathbf{S_{ass}}$. Extract regional state distribution vectors ($\mathbf{r_{ref}}$ and $\mathbf{r_{ass}}$, respectively) and local state distribution vectors ($\mathbf{L_{ref}}$ and $\mathbf{L_{ass}}$, respectively).

$$\mathrm{r}_{\mathrm{ref}} = (r_1^{\mathrm{ref}}, r_2^{\mathrm{ref}}, \ldots, r_N^{\mathrm{ref}}) \tag{6}$$

$$\mathrm{r}_{\mathrm{ass}} = (r_1^{\mathrm{ass}}, r_2^{\mathrm{ass}}, \ldots, r_N^{\mathrm{ass}}) \tag{7}$$

where r_i^{ref} and r_i^{ass} represent the regional state parameter values of the structure reference state and evaluation state at the position of x_i. Remove the overall fluctuations of $\mathbf{r_{ref}}$ and $\mathbf{r_{ass}}$ to get the state changes $\Delta\mathbf{r_{ref}}$ and $\Delta\mathbf{r_{ass}}$.

$$\Delta\mathrm{r}_{\mathrm{ref}} = \mathrm{r}_{\mathrm{ref}} - r_1^{\mathrm{ref}} = (\Delta r_1^{\mathrm{ref}}, \Delta r_2^{\mathrm{ref}}, \ldots, \Delta r_N^{\mathrm{ref}}) \tag{8}$$

$$\Delta\mathrm{r}_{\mathrm{ass}} = \mathrm{r}_{\mathrm{ass}} - r_1^{\mathrm{ass}} = (\Delta r_1^{\mathrm{ass}}, \Delta r_2^{\mathrm{ass}}, \ldots, \Delta r_N^{\mathrm{ass}}) \tag{9}$$

keeping $\Delta\mathbf{r_{ref}}$ constant, multiply $\Delta\mathbf{r_{ass}}$ by the proportionality factor k, and calculate the sum of the state difference between the two for position:

$$df(\Delta\mathrm{r}_{\mathrm{ref}}, k\Delta\mathrm{r}_{\mathrm{ass}}) = \sum_{i=1}^{N} |\Delta r_i^{\mathrm{ref}} - \Delta r_i^{\mathrm{ass}}| \tag{10}$$

where k is a real number, and $df(\Delta\mathbf{r_{ref}}, k\Delta\mathbf{r_{ass}})$ is a state difference function. Find the proportionality coefficient k_0 to minimize the total difference between the reference state and the evaluation state:

$$df(\Delta\mathrm{r}_{\mathrm{ref}}, k_0\Delta\mathrm{r}_{\mathrm{ass}}) = df_{\min}(\Delta\mathrm{r}_{\mathrm{ref}}, k\Delta\mathrm{r}_{\mathrm{ass}}) \tag{11}$$

then normalize $\Delta\mathbf{r_{ref}}$ and $k_0\Delta\mathbf{r_{ass}}$ simultaneously.

$$\mathrm{r}_{\mathrm{ref,norm}} = \frac{\Delta \mathrm{r}_{\mathrm{ref}}}{\max_{i=1,2,\cdots,N}(|\Delta r_i^{\mathrm{ref}}|, |k\Delta r_i^{\mathrm{ass}}|)} = (r_1^{\mathrm{ref,norm}}, r_2^{\mathrm{ref,norm}}, \ldots, r_N^{\mathrm{ref,norm}}) \tag{12}$$

$$\mathrm{r}_{\mathrm{ass,norm}} = \frac{\Delta \mathrm{r}_{\mathrm{ass}}}{\max_{i=1,2,\cdots,N}(|\Delta r_i^{\mathrm{ref}}|, |k\Delta r_i^{\mathrm{ass}}|)} = (r_1^{\mathrm{ass,norm}}, r_2^{\mathrm{ass,norm}}, \ldots, r_N^{\mathrm{ass,norm}}) \tag{13}$$

$\mathbf{r_{ref,norm}}$ is defined as the regional distribution pattern vector of the reference state, and the value range of $[-1,1]$ represents the parameter of the reference state distribution pattern of the structure. $\mathbf{r_{ass,norm}}$ is defined as the parameter of the evaluation state distribution mode, and the value range is [-1,1], which represents the parameter of the evaluation state distribution mode of the structure at the position x_i. The regional distribution pattern matching coefficient at the position of structure x_i is:

$$p_r^i = 1 - \frac{1}{2}|r_i^{\mathrm{ref,norm}} - r_i^{\mathrm{ass,norm}}|, \quad i = 1, 2, \ldots, N \tag{14}$$

The value of p_r^i is [0,1]. The closer the value is to 1, the higher the degree of pattern matching, the more similar the regional distribution pattern of the reference state at the xi position and the regional distribution pattern of the evaluation state.

2.4 Structural Abnormality Recognition Method

In the distributed optical fiber monitoring of civil infrastructures, the criteria for judging the abnormal state of its structure follow the following procedures and basic guidelines.

Step 1 Determine the structural reference state distribution vector $\mathbf{S_{ref}}$ and the evaluation state distribution vector $\mathbf{S_{ass}}$, and unify the measurement point position vector $\mathbf{X}$.
Step 2 Extract the global and local state features respectively. The overall state feature is the regional state distribution vector $\mathbf{r}$ and the local state feature is the local state distribution feature vector $\mathbf{L}$.
Step 3 Identify the region abnormal state of the structure. Firstly, calculate the regional state difference $\Delta\mathbf{r}$.

$$\Delta \mathrm{r} = \mathrm{r}_{\mathrm{ref}} - \mathrm{r}_{\mathrm{ass}} = ((r_1)_{\mathrm{ref}} - (r_1)_{\mathrm{ass}}, (r_2)_{\mathrm{ref}} - (r_2)_{\mathrm{ass}}, \ldots, (r_N)_{\mathrm{ref}} - (r_N)_{\mathrm{ass}}) \tag{15}$$

where $(r_i)_{\mathrm{ref}}$ and $(r_i)_{\mathrm{ass}}$ respectively represent the reference state and evaluation state of the measurement point i in the regional state distribution. $\Delta\mathbf{r}$ reflects the difference between the evaluation status and reference status of each position of the structure. Set the regional state difference abnormality determination threshold k_r, if the elements in $\Delta\mathbf{r}$ satisfy the condition $(r_i)_{\mathrm{ref}} - (r_i)_{\mathrm{ass}} \geq k_r$, then it is determined that the state parameter of the structural position x_i is abnormal. Secondly, calculate the region distribution pattern matching coefficient vector $\mathbf{Pr}$, and set the region state distribution pattern abnormality determination threshold value k_{pr}, if the elements in $\mathbf{Pr}$ meet the conditions $p_r^i \leq k_{pr}$, then it is determined that the regional state distribution pattern of the structural position x_i is abnormal.
Step 4 Identify the local abnormal state of the structure. Firstly, calculate the local state difference $\Delta\mathbf{L}$.

$$\Delta \mathrm{L} = \mathrm{L}_{\mathrm{ref}} - \mathrm{L}_{\mathrm{ass}} = ((l_1)_{\mathrm{ref}} - (l_1)_{\mathrm{ass}}, (l_2)_{\mathrm{ref}} - (l_2)_{\mathrm{ass}}, \ldots, (l_N)_{\mathrm{ref}} - (l_N)_{\mathrm{ass}}) \tag{16}$$

where $(l_i)_{\text{ref}}$ and $(l_i)_{\text{ass}}$ respectively represent the reference state and evaluation state of the measurement point i in the local state distribution. $\Delta\mathbf{L}$ reflects the amount of difference between the estimated state and the reference state at each location of the structure. Set the local state difference anomaly determination threshold value k_{pr}, if the elements in $\Delta\mathbf{L}$ satisfy the condition $(l_i)_{\text{ref}} - (l_i)_{\text{ass}} \geq k_l$, then it is determined that the local state distribution pattern of the structural position x_i is abnormal.

3 Structral Control Method

Under a load condition, the result of the strain distribution at each position using distributed optical fiber measurement is $\mathbf{S_{fiber}}$, and the design allowable strain distribution at each position calculated using the structural design model is $\mathbf{S_{design}}$.

$$\mathrm{S}_{\text{fiber}} = (\, sf_1 \;\; sf_2 \;\; \cdots \;\; sf_N \,) \tag{17}$$

$$\mathrm{S}_{\text{design}} = (\, sd_1 \;\; sd_2 \;\; \cdots \;\; sd_N \,) \tag{18}$$

Feature extraction and analysis of fiber measurement results $\mathbf{S_{fiber}}$, structural regional strain distribution $\mathbf{r_{fiber}}$:

$$\mathrm{r}_{\text{fiber}} = (\, rf_1 \;\; rf_2 \;\; \cdots \;\; rf_N \,) \tag{19}$$

where r_{fi} represents the actual state strain value of the x_i position. $\mathbf{S_{design}}$ is the regional designed strain distribution derived from the structural design calculation. Taking $\mathbf{S_{design}}$ as the object, the full-scale region of the structure is divided into a strain response sensitive region $\mathbf{x_b}$ and a strain response insensitive region $\mathbf{x_s}$:

$$x_{\text{b}} = \left\{ x_i \middle| \left| sd_i \right| > \varepsilon_0, \quad i = 1, 2, \ldots N \right\} \tag{20}$$

$$x_{\text{s}} = \left\{ x_i \middle| \left| sd_i \right| \leq \varepsilon_0, \quad i = 1, 2, \ldots N \right\} \tag{21}$$

The region where the absolute value of the structure design strain response is bigger than ε_0 is determined as the strain response sensitive region, otherwise it is the strain response insensitive region. $\mathbf{x_b}$ represents the region where the strain response value is large under the corresponding load condition, and $\mathbf{x_s}$ represents the region where the strain response value is small. For the strain response sensitive region, the strain value safety factor is defined as following:

$$k_{\text{rb}}^{i} = \frac{rf_i}{sd_i} \tag{22}$$

k_{rb}^{i} represents the ratio of the actual strain response value and the design allowable strain response value at the position x_i of the structure strain response sensitive region. For the strain response insensitive region, the strain value safety factor k_{rs}^{i} is determined in the same way as for the sensitive region. Extract the strain coefficient safety factor abnormal position and composition set for all region of the structure x_{r}:

$$x_{\text{r}} = \left\{ x_i \middle| k_{\text{rb}}^{i} > 1 \vee k_{\text{rb}}^{i} < 0 \vee k_{\text{rs}}^{i} > 1, \quad i = 1, 2, \ldots N \right\} \tag{23}$$

Regional strain distribution pattern matching analysis is performed on $\mathbf{r}_{\mathbf{fiber}}$ and $\mathbf{S}_{\mathbf{design}}$ to evaluate the location of abnormal strain distribution patterns. Regional strain distribution pattern matching coefficient distribution $\mathrm{p_r}$ at each position over the full length:

$$\mathrm{p_r} = (\, p_{\mathrm{r}}^1 \;\; p_{\mathrm{r}}^2 \;\; \cdots \;\; p_{\mathrm{r}}^N \,) \tag{24}$$

In the structural safety assessment, if the three indicators, k_{l}^i, k_{r}^i and p_{r}^i are within the normal value range, the structural state at the x_i position is considered normal; otherwise, if any of the indicators is abnormal, the structural state at the x_i position is considered abnormal. In order to evaluate the threat degree of structural abnormality to structural safety, the safety state risk factor is defined as following:

$$q_a^i = \alpha_i \times k_{\mathrm{r}}^i \times \frac{1}{p_{\mathrm{r}}^i} \times k_{\mathrm{l}}^i \tag{25}$$

$$\alpha_i = \frac{|sd_i|}{\max_{t=1,2,\ldots,N}\{|sd_i|\}} \tag{26}$$

α_i is the risk weight coefficient, which represents the ratio of the design strain response value at the position x_i to the maximum strain response value of the entire length. The larger the value of α_i, the higher the risk weight at the position x_i. k_{r}^i represents the regional strain value safety factor. The larger the value of k_{r}^i, the greater the threat to the structural state safety. $1/p_{\mathrm{r}}^i$ represents the inverse of the matching coefficient of the strain distribution pattern of the structure. The smaller the value of p_{r}^i, the greater the difference between the regional strain distribution pattern and the design. k_{l}^i represents the local strain value safety factor. When $k_{\mathrm{l}}^i > 1$, it represents the local strain is abnormal, and the safety risk of the structure increases. q_α^i represents the threat degree to structural safety caused by abnormal state at the position of x_i. When $q_\alpha^i > 0$, the bigger the value, the greater the risk of structural state at the position of x_i.

4 Smart Safety Monitoring System with Brillouin Distributed Fiber Optic Sensors

A long-span steel structure roof of a high-speed railway station is utilized as the safety monitoring object. The structure is a quadrangular pyramid steel truss with a total length of 1100 m. In order to accurately obtain the global strain distribution of the structure, on the basis of determining a suitable long-distance strain measurement method, it is necessary to study the method of laying out the sensing optical fiber, which matches the actual structure to ensure that the strain measurement method can properly exert measurement effect. For the reason that the sensing fiber can only measure the strain variation along axial direction, and large-span truss structures is primarily under unidirectional stress, the main direction of strain is the focus of safety monitoring. Considering the measurement characteristics of spatial resolution, the sensing fibers need to be in continuous contact with the structure for effective measurement in BOTDA system. Therefore, the sensing fibers are bonded on the surface of the structure with an adhesive, and the contact surface between the fiber and the structure is flat. The fluidity of the adhesive should be better, and the curing time should be longer to avoid uneven thickness of the adhesive layer. The thickness of the sensing fiber

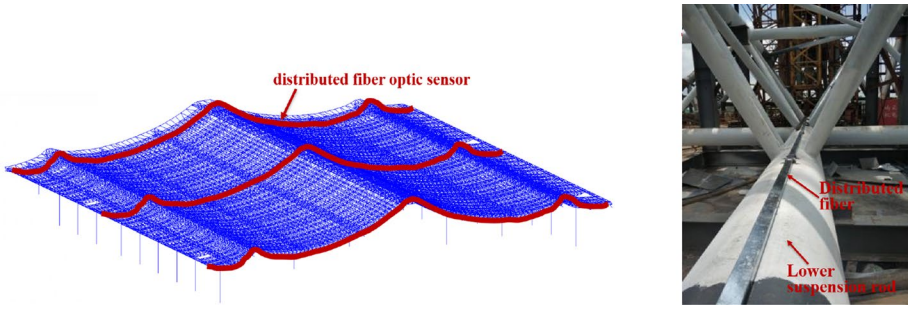

Fig. 4 Location of distributed fiber optic sensor in long-span steel structure

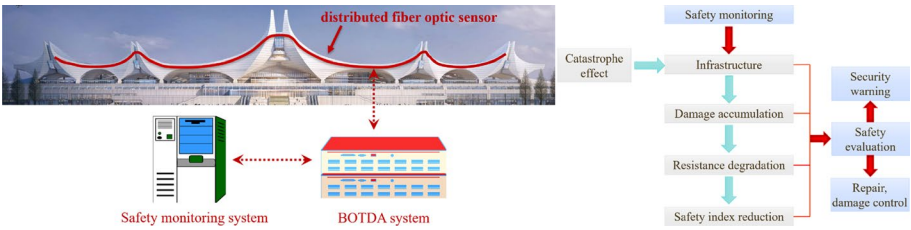

Fig. 5 The framework of the smart safety monitoring and decision system

protective layer is minimized to improve the strain transmission efficiency of the structure and the fiber core.

In accordance with the above principles, a tight-packed strained optical fiber with a diameter of 0.9 mm was employed, and the optical fiber was installed on the upper suspension rod and lower suspension rod of the truss using an epoxy surface bonding method. The specific placement position of the sensing fiber is shown in Fig. 4. Three trusses with large forces were selected and a total of nine sensing fibers were arranged along the length of the structure. Each single-mode fiber with a length of 3500 m covered a sensing distance of 1100 m. The fiber-optic circuit is formed by reciprocating layout and measured using a BOTDA system. The temperature-sensing fiber was in a free state, without adhesive sticking. It was arranged close to the strain-sensing fiber and covers the same monitoring range. Nine sensing optical fibers and the demodulation system work together to form a long-span steel structure distributed optical fiber strain monitoring system. The framework and function of the monitoring system are shown as Fig. 5.

5 Verification of the AI-Based Self-Learning System

The safety condition of the structure was evaluated based on the measurement results of full-scale strain distribution. In order to determine the design allowable strain distribution of the structure, a finite element model of the structure design was established, and the calculation result of the full-scale strain distribution of the structure corresponding to each load test (2 t static load) was used as the design allowable strain distribution. All structural members such as the upper suspension rods, the lower suspension rods, and diagonal web

members of the structure were simulated by beam elements, and the restraint mode was constrained by nodes. The component materials of the structure are Q345 steel, the elastic modulus is 2.01×10^5 MPa, the Poisson ratio is 0.3, and the design yield strength is 300 MPa. Finite element software ABAQUS was utilized to run the finite element model of the structure, as shown in the Fig. 6. The allowable structural strain distribution results of the structure design corresponding to each load condition calculated by the finite element model are shown in Fig. 7, and compared with the measurement results of distributed fiber and the single-point measuring by fiber bragg frating (FBG) strain sensors.

The consistency of the measurement results of the distributed optical fiber and the grating strain gauge shows the accuracy of the actual strain state measurement of the structure. The design allowable strain value is generally greater than the actual structure strain value, for the reason that the design model takes into account the safety factor of the structure. The contour shape of the design strain distribution corresponding to each load case is the same as the actual strain distribution. Under axisymmetric loading (case 4 in Fig. 7), since the structure is designed and constructed according to symmetrical geometric dimensions, material parameters, structure and boundary conditions, the strain response is symmetrically distributed along the length direction under the action of axisymmetric loading. The single-point strain in Fig. 7 is from FBG(Fiber Bragg Grating) strain sensor at corresponding position. The design strain distribution and the actual strain distribution of the structure are symmetrical, and the areas where positive and negative strains appear are the same, which indicates that the symmetry of the strain distribution is good, and the strain distribution mode is consistent with that of design result.

The allowable strain distribution data of the structure design was set to $\mathbf{S}_{\mathbf{design}}$, and the measured strain distribution data of the distributed fiber is set to $\mathbf{S}_{\mathbf{fiber}}$ to evaluate the structural abnormal state. Firstly, the abnormal position of the strain response value in the structure was evaluated. The strain threshold ε_0 was set to 50με, the classify of the structure position into the strain response sensitive area and strain response insensitive area was carried out, the distribution feature extraction window length w_a was set to 5 m, the strain distribution $\mathbf{r}_{\mathbf{fiber}}$ was extracted, and the safety factor k_r in the full-scale structure was calculated and shown as dot dash line in Fig. 8. It can be seen that the safety factor of the regional strain value in full-scale of the structure under the four load test case conditions is in the range of (0,1), which is in the safe value range. Secondly, based on $\mathbf{r}_{\mathbf{fiber}}$ and $\mathbf{S}_{\mathbf{design}}$, the actual and design region strain distribution patterns of the truss were extracted, and the region distribution pattern matching coefficient p_r was calculated and shown as dotted line in Fig. 8. The regional strain distribution pattern matching threshold p_0 was set to 0.9. It can be seen that the values of p_0 of all positions in the four load test case conditions are in the range of (0.95,1). The actual strain

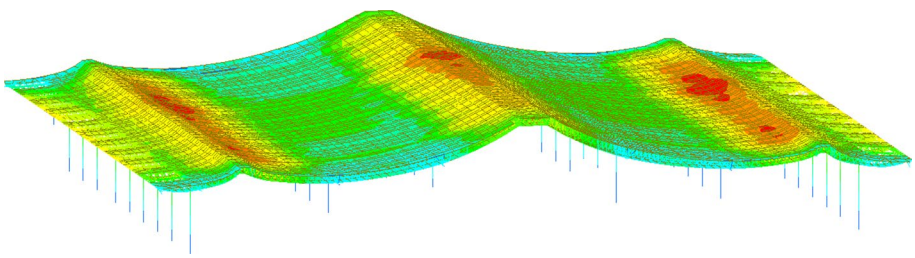

Fig. 6 Strain distribution of the structure in finite element model simulations

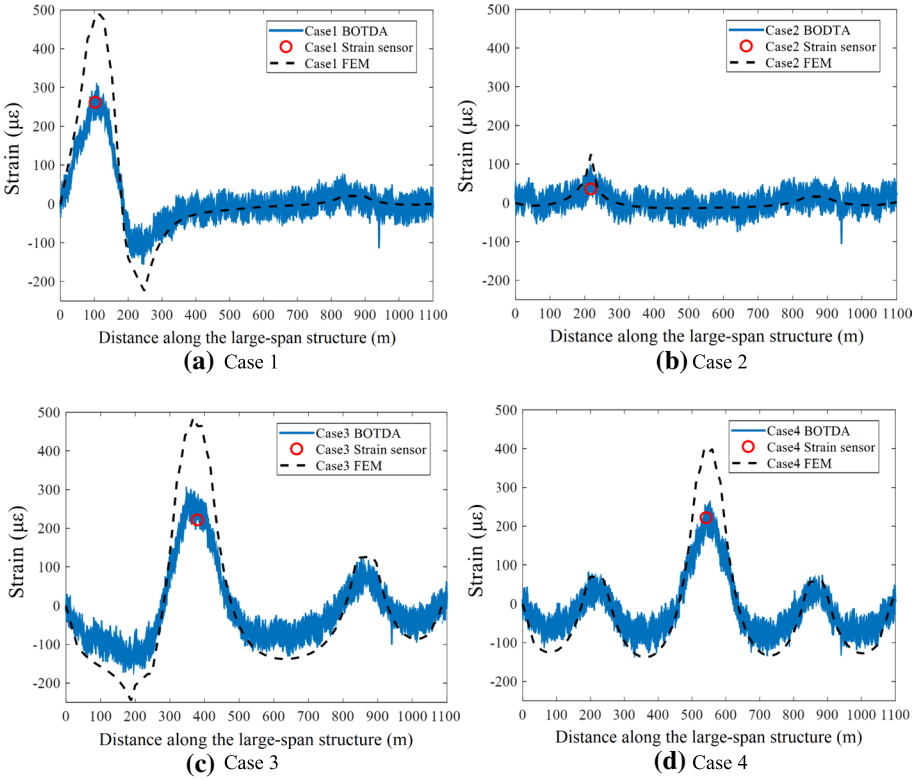

Fig. 7 Comparisons of strain distributions of structure between safety assessment results and FEM simulations results

distribution pattern of the structure is consistent with the design, and the operating mode of the structural mechanics system meets the design requirements. It can be seen that k_l of the full-scale structure under the four load test case conditions are in the range of (0,1), which means in the safe value range. The results indicate that the local strain fluctuations of structure are less than the allowable strain value. There is no significant local strain fluctuation caused by local damage such as cracks, warping, corrosion, etc., therefore, the behaviour of the whole structure is normal.

Considering no abnormal position of the strain state in full length of the structure, there is no comparison of the degree of the threat of the strain abnormal position to the safety of the bridge structure. In order to show the calculation results of the safety state assessment method and provide a reference for the assessment of the safety state of the structure after several years of service in the future, the structure safety state risk factor q_{a} is shown in Fig. 9. It can be seen that the values of q_{a} of the structure under each load test condition is in the range of (0,0.6). The values in the high strain region are significantly larger than that of the low strain region, which is consistent with actual condition. For the calculation result of the risk factor at the position x_i in the normal state, the magnitude of the value represents the degree of threat to the structure safety due to the change of the strain state. More importantly, the calculation result of q_{a} can also be used as a reference for subsequent structural safety assessment. When the risk factor

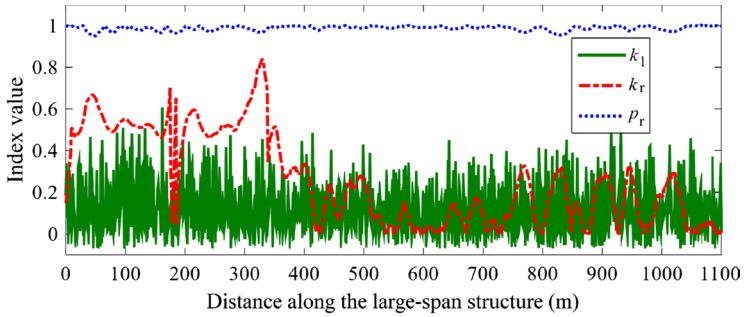

(a) Case 1

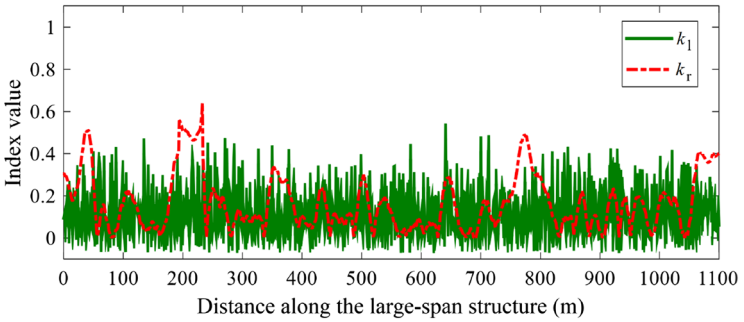

(b) Case 2

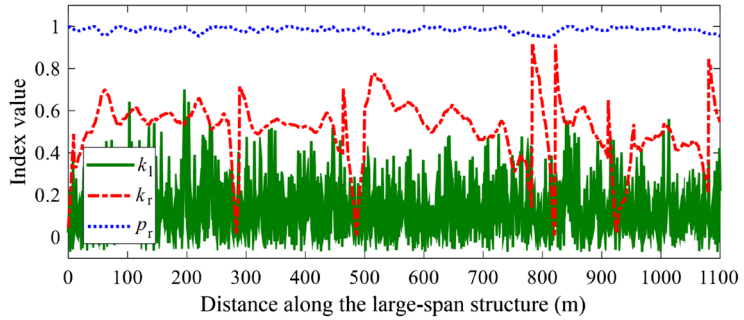

(c) Case 3

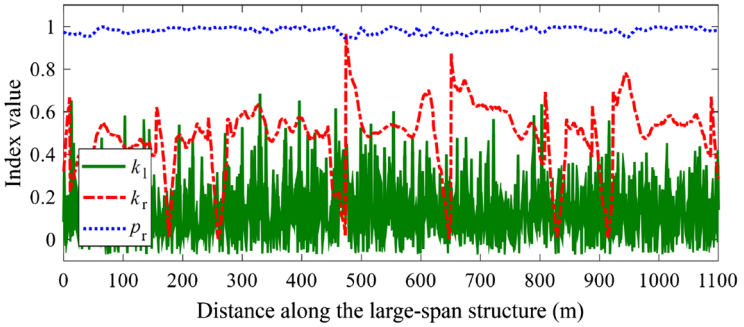

(d) Case 4

Fig. 8 Damage assessment results along the full length of the structure

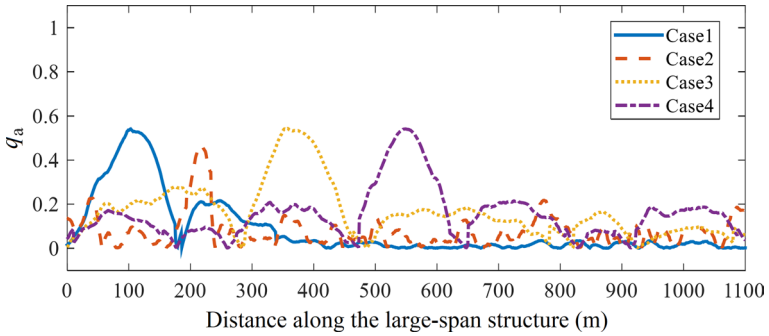

Fig. 9 Risk factor along the full length of the structure

gradually increases with time in certain region, it means that the structural performance degenerates and the structural safety risk increases.

6 Conclusions

This paper presents an innovative method for distributed structural health and control systems based on artificial intelligence. The system contains feature extraction and characterization for distributed structural behaviours, pattern matching for evaluating structural response distributions, structural abnormality recognition, safety monitoring and condition assessment for civil infrastructures. The applicability of the method was verified by actual engineering load test and FE simulation analysis. The following conclusions are drawn based on the outcomes of this study.

1. The full-scale distributed fiber measurement results can be separated into regional and local condition distribution. Each condition distribution contains two types of information: condition parameter values and distribution patterns, which can be used to identify structural abnormality or damage at multiple levels. The separation and matching method of structural condition proposed in this paper can effectively separate the global and local state characteristics of the structure and identify abnormal condition.
2. The method of structural safety monitoring forthputting intelligent distributed fiber optic monitoring information can effectively avoid the missing out of the location related to abnormal response, solve the problem of insufficient sensing capabilities in huge civil infrastructures. The reliability of monitoring results is improved significantly.
3. Comparing with the results of discrete FBG monitoring and FE simulation analysis, it is shown that AI-based self-learning system could offer suitable speed in deployment, reliability in solution and flexibility to adjust in distributed structural health monitoring and control..

Funding This study was funded by the Shandong Key Research and Development Plan (Grant: 2018GSF120006).

Declarations

Conflict of interest The authors declare that they have no conflict of interest.

References

1. Ravet F, Bao XY, Chen L (2004) Effect of pulsewidth on strain measurement accuracy in Brillouin-scattering-based fiber optic sensors. SPIE 5579:187–194
2. Wu ZS, Xu B, Hayashi KJ et al (2006) Distributed optic fiber sensing for a full-scale PC girder strengthened with prestressed PBO sheets. Eng Struct 28:1049–1059
3. Xu J, He JP, Zhang L (2017) Collapse prediction of karst sinkhole via distributed Brillouin optical fiber sensor. Measurement 100:68–71
4. Sperber T, Eyal A, Tur M et al (2010) High spatial resolution distributed sensing in optical fibers by Brillouin gain-profile tracing. Opt Express 18(8):8671–8679
5. Xu ZN, Zhao LJ (2020) Estimation of error in Brillouin frequency shift in distributed fiber sensor. IEEE Sens J 20(4):1829–1837
6. Chan THT, Yu L, Tam HY et al (2006) Fiber Bragg grating sensors for structural health monitoring of Tsing Ma bridge: background and experimental observation. Eng Struct 28(5):648–659
7. Taki M, Soto MA, Bolognini G et al (2013) Study of Raman amplification in DPP-BOTDA sensing employing simplex coding for sub-meter scale spatial resolution over long fiber distances. Meas Sci Technol 24(9):94–108
8. Rodriguez G, Casas JR, Villalba S (2015) SHM by DOFS in civil engineering: a review. Struct Monit Maint 2(4):357–382
9. Soto MA, Bolognini G, Di Pasquale F (2010) Analysis of pulse modulation formatnin coded BOTDA sensors. Opt Express 18(14):14878–14892
10. Kishida K, Li C (2005) Pulse pre-pump-BOTDA technology for new generation of distributed strain measuring system. Struct Health Monit Intell Infrastruct 1:471–477
11. Zhou Z, He JP, Ou JP (2008) Long-term monitoring of a civil defensive structure based on distributed Brillouin optical fiber sensor. Pac Sci Rev 8:1–6
12. Kim YH, Song KY (2017) Tailored pump compensation for Brillouin optical time-domain analysis with distributed Brillouin amplification. Opt Express 25(13):14098–14105
13. Bao X, Dhliwayo J, Heron N et al (1995) Experimental and theoretical studies on a distributed temperature sensor based on Brillouin scattering. J Lightwave Technol 13(7):1340–1348
14. Glisic B, Inaudi D (2011) Development of method for in-service crack detection based on distributed fiber optic sensors. Struct Health Monit 11(2):161–171
15. Leung CKY, Wan KT, Inaudi D et al (2015) Review: optical fiber sensors for civil engineering applications. Mater Struct 48(4):871–906
16. Minardo A, Coscetta A, Porcaro G et al (2015) Structural health monitoring in the railway field by fiber-optic sensors. In: Compagnone D, Baldini F, Di Natale C, Betta G, Siciliano P (eds) Sensors. Springer, Berlin, pp 359–363
17. Li S, Zhu S, Xu YL et al (2012) Long-term condition assessment of suspenders under traffic loads based on structural monitoring system: application to the Tsing Ma bridge. Struct Control Health Monit 19(1):82–101

18. Zhang D, Shi B, Cui HL et al (2004) Improvement of spatial resolution of Brillouin optical time domain reflectometer using spectral decomposition. Opt Appl 34(2):291–301
19. Zhou Z, He JP, Yan K, Ou JP (2008) Fiber-reinforced polymer-packaged optical fiber sensors based on Brillouin optical time-domain analysis. Opt Eng 47(1):1–10
20. Angulo VX, Martin LS, Corredera P et al (2012) Raman-assisted Brillouin optical time-domain analysis with sub-meter resolution over 100 km. Opt Express 20(11):12147–12154
21. Iten M, Puzrin AM (2009) BOTDA road-embedded strain sensing system for landslide boundary localization. In: Proceedings of SPIE 7293, Smart Sensor Phenomena, Technology, Networks, and Systems, pp 729312–729316
22. Dong C, Ding H, Gao S (2002) A method for recognition and localization of structural damage. Struct Mech 30(2):193–201
23. Koyamada Y, Sakairi Y, Takeuchi N (2007) Novel technique to improve spatial resolution in Brillouin optical time-domain reflectometry. IEEE Photonics Technol Lett 19(23):1910–1912
24. Ravet F, Zou LF, Bao XY et al (2004) Demonstration of the detection of buckling effects in steel pipelines and beams by the distributed Brillouin sensor. Proc SPIE 5579:58–65
25. Bai Y, Xing JC, Xie F, Liu SJ, Li JX (2019) Detection and identification of external intrusion signals from 33 km optical fiber sensing system based on deep learning. Opt Fiber Technol 53:1–9
26. Soto MA, Taki M, Bolognini G et al (2012) Optimization of a DPP-BOTDA sensor with 25cm spatial resolution over 60km standard single-mode fiber using simplex codes and optical pre-amplification. Opt Express 20(7):6860–6869
27. Sienko R, Zych M, Bednarski L (2019) Strain and crack analysis within concrete members using distributed fibre optic sensors. Struct Health Monit Int J 18(5–6):1510–1526
28. Van DK, Hoult NA (2018) Assessment of a steel model truss using distributed fibre optic strain sensing. Eng Struct 171:557–568
29. Bao Y, Tang F, Chen Y et al (2016) Concrete pavement monitoring with PPP-BOTDA distributed strain and crack sensors. Smart Struct Syst 18(3):405–423
30. Arhant M, Meek N, Penumadu D (2018) Residual strains using integrated continuous fiber optic sensing in thermoplastic composites and structural health monitoring. Exp Mech 58(1):167–176